Journal of BUON **13:** 75-86, 2008
© 2008 *Zerbinis Medical Publications. Printed in Greece*

ORIGINAL ARTICLE

Comparison of the 3D-conformal, helical tomotherapy and multileaf collimators-based intensity modulated radiotherapy modalities using radiobiological measures

P. Mavroidis[1,2], B. Costa Ferreira[1,3], C. Shi[4,5], B.K. Lind[1], N. Papanikolaou[4,5]

[1]Department of Medical Radiation Physics, Karolinska Institutet and Stockholm University, Stockholm, Sweden; [2]Department of Medical Physics, Larissa University Hospital, Larissa, Greece; [3]I3N Physics Department, University of Aveiro, Aveiro, Portugal; [4]Department of Radiation Oncology, University of Texas Health Science Center, San Antonio TX, USA; [5]Department of Medical Physics, Cancer Therapy and Research Center, San Antonio TX, USA

Summary

Purpose: *Intensity modulated radiotherapy (IMRT) using multileaf collimators (MLC) and helical tomotherapy (HT) have become increasingly popular over the past few years. However, their clinical efficacy and effectiveness continue to be investigated. In order to provide a more thorough evaluation and comparison of treatment plans, the utilization of the biologically effective uniform dose ($\bar{\bar{D}}$) together with the complication-free tumor control probability (P_+) are examined.*

Materials and methods: *In this study, a typical case of lung cancer was investigated by developing a 3D conformal treatment plan, a linac MLC-based step-and-shoot IMRT plan and a HT plan. The 3 different treatment plans were compared based on radiobiological measures by using the P_+ index and the $\bar{\bar{D}}$ concept as the common prescription point of the plans and plotting the tissue response probabilities vs. $\bar{\bar{D}}$ for a range of prescription doses.*

Results: *The applied plan evaluation method showed that in this lung cancer case the MLC-based IMRT plan was best over the clinically useful dose prescription range. The 3D-conformal, MLC-based IMRT and HT treatment plans gave a P_+ of 55.4%, 72.9% and 66.9%, for a $\bar{\bar{D}}$ to the internal target volume (ITV) of 57.0 Gy, 66.9 Gy and 64.0 Gy, respectively.*

Conclusion: *In comparison to 3D conformal radiotherapy, both MLC based-IMRT and HT can better encompass the often large ITV required while minimizing the volume of the organs at risk receiving high dose. Taking into account the dose-response relations of the irradiated tumors and normal tissues, a radiobiological treatment plan evaluation can be performed, which may provide a closer association of the delivered treatment with the clinical outcome.*

Key words: biologically effective uniform dose, conformal radiotherapy, complication-free tumor control, dose-response relations, helical tomotherapy, radiobiological evaluation

Introduction

The low tolerance doses, which characterize the involved organs-at-risk (OAR), are usually the major constraints in radiation therapy. The dose delivered to the frequently massive tumors is further limited when these OARs are in close proximity to the gross tumor volume (GTV) and clinical target volume (CTV) [1,2]. It has been demonstrated that IMRT can significantly reduce radiation dose and toxicity to critical organs producing better results than conventional and simple conformal radiation therapy techniques [3]. Today, there are several treatment planning systems (TPS) available for performing physical IMRT optimization. The selection of the best treatment plan can be a challenging task due to variations in the optimization methodology, which may lead to discrepancies between integral doses and expected response probabilities.

Isodose distribution, dose volume histogram (DVH) and maximum, minimum, mean and standard deviation of a dose distribution, are currently the main concepts for radiotherapy treatment plan evaluation. However, all these evaluation tools are only dose-based and they do not take the radiobiological characteristics

Correspondence to: Panayiotis Mavroidis, PhD. Department of Medical Radiation Physics, Karolinska Institutet and Stockholm University, Box 260, S-171 76 Stockholm, Sweden. Tel: +30 2410 682865, E-mail: panayiotis.mavroidis@radfys.ki.se

Received 14-07-2007; Accepted 04-10-2007

of tumors or normal tissues into account. In some situations, competing plans are characterized by significantly different radiobiological outcomes even though they have similar mean, maximum and minimum doses [4]. To deal with these cases, the use of the biologically effective uniform dose ($\bar{D}$) and complication-free tumor control (P_+) have been proposed as alternative plan evaluation tools [5]. The concept of biologically effective uniform dose, $\bar{D}$ assumes that any two dose distributions are equivalent if they cause the same probability for tumor control or normal tissue complication [4]. The $\bar{D}$ concept makes use of the fact that probabilities averaged over both dose distribution and organ radiosensitivity are more relevant to the clinical outcome.

HT is a recently developed technology for radiation therapy, which is characterized by treatment plans of higher dose conformality than other IMRT techniques [6,7]. In HT technology, radiation is delivered helically through 51 projections per rotation. In the literature, there are reports on the comparison of dose distributions delivered by 3D-conformal and IMRT techniques [8,9]. However, comparison studies between HT and other IMRT modalities are limited. Consequently, the question regarding the comparison of the effectiveness of dose distributions between HT and other radiation therapy modalities, such as that of the linac-based IMRT using MLC in a step-and-shoot mode, still remains.

The goal of this study was to use radiobiological measures in order to compare the 3D-conformal, MLC-based IMRT and HT radiation modalities. For this purpose, a representative case of lung cancer has been evaluated. Two treatment plans have been developed using the Philips (ADAC) Pinnacle TPS and one plan using the HT TPS. The calculation results, such as the maximum, minimum and mean doses, have been collected and the P_+ index together with the $\bar{D}$ dose have been derived and analyzed. To reveal the value of biological and physical factors in assessing treatment plans, a parallel physical and biological evaluation was performed. The implemented radiobiological procedure used the dose-response relations of tumors and surrounding normal tissues to compare the merits of the incident beam profiles and projections and estimate the probability of achieving complication-free tumor control [10-14].

Materials and methods

Treatment planning and delivery units

In this study, a lung cancer case was investigated by developing a linac 3D-conformal treatment plan, a MLC-based step-and-shoot IMRT plan and a HT plan. For this purpose, two IMRT treatment delivery machines were used: a Varian linac 21EX with a dose calculation grid resolution of $3\times3\times3$ mm^3 (Varian Medical Systems, Palo Alto, CA) and a Hi·Art II TomoTherapy (TomoTherapy, Inc. Madison, WI). The Varian linear accelerator model is a 21EX outfitted with a MILLENNIUM 120 leaf MLC. The HT unit has a 64 leaf binary MLC and it has been commissioned for 2.5 and 5.0 cm jaw models. The HT plan is delivered through a helical mode. To produce the sinogram intensity modulation, which is required to achieve the prescribed objectives, the 2.5×40 cm slit beam was modulated by a binary multileaf collimator. The treatment planning system used for the 3D conformal and MLC-based IMRT linear accelerator plans was Pinnacle (ADAC Laboratories, Milpitas, CA, version 7.6c). For the HT plan, the dedicated Tomotherapy treatment planning station, version 2.1.2, was used. The delineation of the target and organs at risk was performed on the Pinnacle planning station and subsequently transferred to the Tomotherapy planning station via the DICOM-RT protocol. The produced dose distributions were subsequently compared by using physical and radiobiological measures.

A CT simulation was performed with the patient in the treatment position using rigid immobilization devices including the region above and below the treatment area. The ITV was created by expanding the gross tumor volume (GTV) with an appropriate margin for organ motion. The dose prescription guidelines and fractionation schedule were the same for all the plans. For the 3D-conformal and MLC-based IMRT plans, all beams were of 6 MV energy, coplanar and equally spaced around the patient. In the end of the treatment planning process, the dose matrix of the HT plan was exported to the Pinnacle workstation for comparative plan analysis and evaluation. The export of the dose matrix from the Tomotherapy TPS and its transfer to the Pinnacle planning station was performed through an in-house developed software tool [15]. This tool assures that the dose matrix and the patient's anatomy are correctly aligned and scaled.

The linac-based step-and-shoot IMRT plan was optimized with direct machine parameter optimization (DMPO). For initial setup, a protocol was developed in the HT treatment plan optimization. The jaw setting was selected as 2.5 cm, the pitch value was set to 0.287, and the modulation factor was set to 2.0 for this treatment site. For tumors, the importance value was set to 50, maximum and minimum dose penalties were set to 100. For organs at risk, the importance value was set to 15, maximum dose penalty was set to 1 and minimum dose penalty was set to 20. The optimization criteria were used to adjust the final plan values for impor-

tance, maximum and minimum dose penalties. After the completion of the optimization, the same physician reviewed the dose-volume histograms and isodose distributions for final approval of the treatment plans. For all the 3 treatment plans, the values of relevant statistical parameters such as maximum, minimum and mean doses as well as irradiated normal tissue volume and density were collected for analysis.

Treatment plan criteria and prescription

The final approval of the treatment configurations was based on the following general clinical criteria: 1) uniform dose to the ITV (with a standard deviation less than 5%); 2) minimum dose to the surrounding healthy tissue stroma; and 3) minimum dose to the organs at risk (below equation 1 describes their respective tolerance doses). More specifically, a 46-year-old patient with metastatic adenocarcinoma of the lung was planned to be treated. A dose prescription of 60 Gy in 30 fractions, giving 200 cGy/fraction was applied. The basic characteristics of the 3 treatment plans are:

- 4 field conformal plan: AP, RAO, RPO, and PA beams
- MLC-based IMRT treatment plan: 6 coplanar beams of 6MV energy were delivered at gantry angles of 330, 230, 180, 130, 30, 10 degrees.
- Tomotherapy plan used a pitch of 0.3 and 2.5 width jaw setting.

All calculations were performed using the convolution/superposition dose calculation algorithm that accounts for density inhomogeneity effects [16,17].

Radiobiological treatment plan evaluation

In this study, the dose-response relations of the tumors and normal tissues are described by the Linear-Quadratic-Poisson model [18,19]. This model can take into account the fractionation effects that are introduced by the irradiation schedule:

$$P(D) = \exp\left(-e^{e\gamma-\alpha nd-\beta nd^2}\right) \approx \exp\left(-e^{e\gamma-(D/D_{50})\cdot(e\gamma-1n1n2)}\right) \quad (1)$$

where $P(D)$ is the probability to control the tumor or induce a certain injury to a normal tissue that is irradiated uniformly with a dose D, $d = D/n$ is the dose per fraction and n is the number of fractions. The variables α and β are the fractionation parameters of the model and account for the expected early and late effects, respectively. D_{50} is the dose, which gives a 50% response and γ is the maximum normalized dose-response gradient. N_0 is the initial number of the clonogenic cells for tumors or functional subunits (FSU) for healthy tissues. Parameters D_{50} and γ are specific for every organ and type of clinical endpoint and they can be calculated from the α and β variables or be derived directly from clinical data [13,14,20-22]. When the values of the D_{50} and γ parameters are derived from clinical materials, the dose distributions have to be corrected for the fractionation effects, which means that the knowledge of the α/β ratio is necessary. The response of the entire organ to a non-uniform dose distribution is given by an expanded version of equation 1 for tumors and the relative seriality model for normal tissues [22].

The response of a normal tissue to a non-uniform dose distribution is given by the relative seriality model. This model accounts for the volume effect. For a heterogeneous dose distribution, the overall probability of injury P_I (I denotes injury) [19,22] for a number of OARs is expressed as follows:

$$P_I = 1-\prod_{j=1}^{N_{organs}}\left(1-P_I^j\right) = 1-\prod_{j=1}^{N_{organs}}\left(1-[1-\prod_{i=1}^{M_j}(1-P^j(D_i)^{s_j})^{\Delta v_i}]^{1/s_j}\right) \quad (2)$$

where P_I^j is the probability of injuring organ j and N_{organs} is the total number of vital OARs. $P^j(D_i)$ is the probability of response of the organ j having the reference volume and being irradiated to dose D_i as described by equation 1 $\Delta v_i = \Delta V_i / V_{ref}$ is the fractional subvolume of the organ that is irradiated compared to the reference volume for which the values of D_{50} and γ have been calculated. M_j is the total number of voxels or subvolumes in the organ j, and s_j is the relative seriality parameter that characterizes the internal organization of that organ. $s \approx 1$ corresponds to a completely serial structure which becomes non-functional when at least one functional subunit is damaged, whereas $s \approx 0$ corresponds to a parallel structure, which becomes non-functional when all its functional subunits are damaged.

In tumors, the structural organization is assumed to be parallel since the eradication of all their clonogenic cells is required. Furthermore, in complex multi-target cancer cases, the eradication of every individual tumor has to be achieved. This pattern indicates that the different targets are related through a parallel organization fashion. Taking these features into account the overall probability of benefit P_B (B denotes benefit from tumor control), is given by the equation:

$$P_B = \prod_{j=1}^{N_{tumours}} P_B^j = \prod_{j=1}^{N_{tumours}}\left(\prod_{i=1}^{M_j} P^j(D_i)^{\Delta v_i}\right) \quad (3)$$

where P_B^j is the probability of eradicating tumor j and $N_{tumours}$ is the total number of tumors or targets involved in the clinical case.

It should be mentioned that other models such as the LKB [23-25], Parallel [26] etc, could also have been used with the appropriate response parameter sets. In Table 1, the dose-response parameters of the organs used in this study are shown. This parameter set is

Table 1. Summary of the model parameter values for the lung cancer case. D_{50} is the 50% response dose, γ is the maximum normalized value of the dose-response gradient and s is the relative seriality, which characterizes the volume dependence of the organ

Relative seriality model	*Parameter values*			
Lung cancer	D_{50} *(Gy)*	γ	s	α/β
ITV*	49.2	1.0	–	10.0
Spinal cord	57.0	6.7	1.0	3.0
Esophagus	68.0	2.8	3.4	3.0
Heart	70.7	0.96	1.0	10.0
Ipsilateral lung	30.1	0.97	0.01	3.0

*internal target volume

based on published data [11-14,20,21,27-30]. For many tissues the values of relative seriality have been determined from clinical data from the work by Emami *et al.* [11], where the relative seriality model was fit on the dose-response diagrams (Ågren 1995) [12]. In certain cases (like esophagus), relative seriality values larger than one have been calculated, which is equivalent to having a serial tissue with so sparsely distributed FSUs that there are voxels without an FSU inside them [19]. The uncertainties that are associated with these parameters are of the order of 5% for D_{50}, 30% for γ and 90% for s. These uncertainties define the confidence interval of the entire dose-response curve around its best estimate [31]. In this study, it was assumed that the patient was of average radiosensitivity, which is characterized by the mean estimates of the radiobiological parameters presented.

The effectiveness of the different treatment plans is evaluated though the concepts of $\bar{\bar{D}}$ and P_+. $\bar{\bar{D}}$ is the biologically effective uniform dose [3,4], whereas P_+ is a scalar quantity which expresses the probability of achieving tumor control without causing severe damage to normal tissues [5]. In the current clinical practice, the quality of a treatment plan is usually assessed through the mean doses and dose variations in the target volumes and organs at risk, together with the respective minimum and maximum doses. In addition to these parameters, the $\bar{\bar{D}}$ concept is used in this study to evaluate the treatment plans. The biologically effective uniform dose is defined as the dose that causes the same tumor control or normal tissue complication probability as the actual dose distribution given to the patient. In the former case the biologically effective uniform dose is denoted as $\bar{\bar{D}}_B$, whereas in the latter case as $\bar{\bar{D}}_I$. The notation $\bar{\bar{D}}$ indicates that the quantity has been averaged over both the dosimetric (dose distribution) and the biological (dose-response relations) information of the clinical case. The general expression of $\bar{\bar{D}}$ is defined, for a given tumor or normal tissue, from its dose-response relation without dependence on the radiobiological model used and it is derived numerically by the first part of the following equation, whereas for a tissue of uniform radiosensitivity, $\bar{\bar{D}}$ is given from the latter analytical equation:

$$P(\vec{D}) \equiv P(\bar{\bar{D}}) \Rightarrow \bar{\bar{D}} = \frac{e\gamma - 1\mathrm{n}(-1\mathrm{n}(P(\vec{D})))}{e\gamma - 1\mathrm{n}(1\mathrm{n}\,2)} \qquad (4)$$

where $\vec{D}$ denotes the 3-dimensional dose distribution. This definition is a generalization and combination of the effective uniform dose, D_{eff} introduced by Brahme [32], and the equivalent uniform dose (EUD) introduced by Niemierko [33]. Using this dose concept, a number of plan trials can be compared based on radiobiological endpoints by normalizing their dose distributions to a common prescription point ($\bar{\bar{D}}$) and then plotting out the tissue response probability vs. $\bar{\bar{D}}$ curves.

In this work, the probability of getting benefit from a treatment (tumor control) is denoted by P_B, whereas the probability for causing severe injury to normal tissues by P_I [3,22]. Using these quantities, P_+ can be estimated from the following equation:

$$P_+ = P_B - P_{B\circ I} = P_B - P_I + \delta\,(1 - P_B)\,P_I \qquad (5)$$

where the parameter δ represents the fraction of the patients with statistically independent tumor and normal tissue responses. A set of clinical data estimated the value of δ being below 20% [18]. The importance of this concept increases with the accuracy of the radiobiological parameters, which describe the dose-response relations of the different tumors and normal tissues since this makes the probabilities P_B and P_I more reliable and clinically relevant. The treatment plans of the study were evaluated radiobiologically using the radiation sensitivities of the tumor and OARs involved although conventional physical criteria like dose volume histograms, isodose charts, etc, were also employed. The objective was to estimate the normal tissue tolerance against the optimum target dose needed [34,35]. An in-house developed software tool was used to calculate the dose volume histograms (DVHs) and the probabilities of benefit and injury as well as the values of the complication-free tumor control probability, P_+ and biologically effective uniform dose, $\bar{\bar{D}}$.

Results

Figure 1 depicts the comparison of the isodose curve distributions of the 3D-conformal, MLC-based IMRT and HT treatment plans, respectively, in transverse and sagittal views of the lung cancer case. In this clinical case, the sensitive organs at risk are the spinal cord, esophagus, heart and ipsilateral lung. Based on

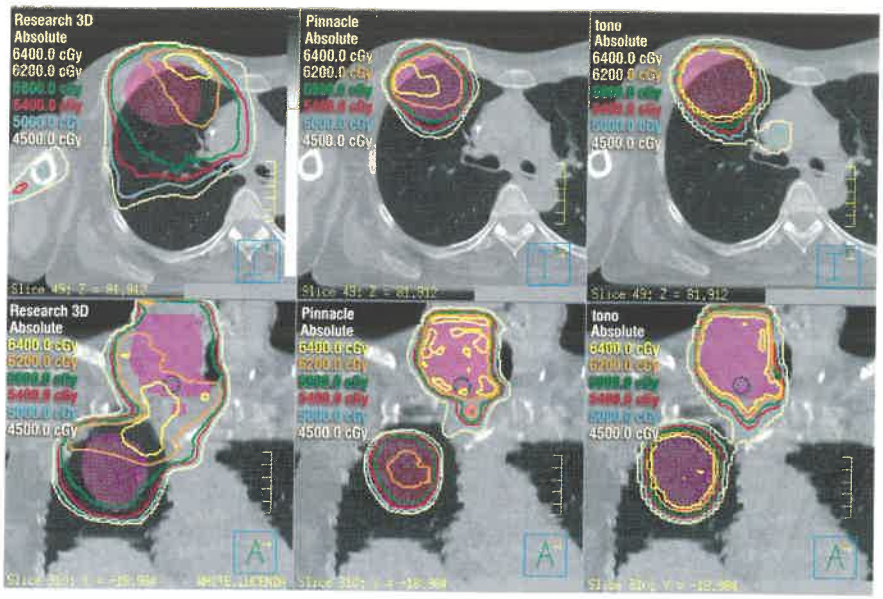


Figure 1. The reference CT slice of a lung cancer patient is shown for the 3D-conformal, MLC-based IMRT and HT treatment plans in transverse and coronal planes. The anatomical structures involved are illustrated together with the applied dose distributions to be delivered to the patient.

the isodose curve distributions, it is clear that the 3D-conformal treatment plan has a quite large dose spread outside the ITV and a moderate inhomogeneity inside the ITV. The HT plan has higher dose spread outside the ITV compared to the MLC-based IMRT but lower inhomogeneity inside the ITV. The mean dose to the ITV was highest in the HT and lowest in the 3D-conformal plan (Table 2). Regarding the organs at risk, the 3D-conformal treatment plan delivers significantly higher doses to the esophagus and lung (33.9 Gy and 19.1 Gy, respectively) compared to the MLC-based IMRT and HT plans. Between the MLC-based IMRT and HT modalities, the former delivers higher doses to the spinal cord and esophagus (22.3 Gy and 23.5 Gy, respectively), whereas the latter delivers higher doses to the heart and lung (6.9 Gy and 15.5 Gy, respectively). It is shown that in all cases the mean dose, $\bar{D}$ to the ITV is very close to the corresponding $\bar{\bar{D}}$ values because of the small dose variations within the ITV. On the contrary, the dose distributions within the OARs are characterized by much larger variations with the largest ones being observed in the 3D-conformal plan for the esophagus and lung (23.5 Gy and 21.8 Gy, respectively). This has a consequence that the $\bar{\bar{D}}$ values of the normal tissues are greater than the corresponding mean doses, $\bar{D}$, especially for the spinal cord, esophagus and heart.

In Figures 2 and 3, the treatment plans are compared in terms of DVHs and dose-response curves. The dose-response curves of the ITV and each organ at risk are presented, together with the P_+ curve. In the upper right diagrams of Figures 2 and 3, the response curves are all normalized to the mean dose in the ITV ($\bar{D}_{ITV}$). In the lower left diagrams of the figures, the dose-response curves have been normalized to the $\bar{\bar{D}}_B$, which forces the response curves of the ITV (P_B) of the different treatment plans to coincide. Finally, in the lower right diagrams of the figures, by normalizing the dose-response curves to the $\bar{\bar{D}}_I$, the total complication response curves (P_I) of the different treatment plans coincide. In these diagrams, the curves show how tissue responses change with dose prescription since the same dose distribution is kept at all dose levels. Intercomparison of the different modalities on the same basis can be performed by using for normalization the concepts $\bar{\bar{D}}_B$ or $\bar{\bar{D}}_I$. This approach gives emphasis to the therapeutic window, which characterizes each treatment plan. A quantitative summary of the physical and biological comparisons is presented in Table 2.

For the planned dose prescription the P_+ value for the 3D-conformal treatment plan is 50.0% for a mean dose to the ITV of $\bar{D}_{ITV} = 61.4$ Gy and biologically effective uniform dose to the ITV, $\bar{\bar{D}}_B$ of 61.3 Gy. The total control probability, P_B, is 72.6% and the total complication probability, P_I, is 22.5%. Similarly, for the MLC-based radiation modality the P_+ value is 70.9% for $\bar{D}_{ITV} = 62.4$ Gy and $\bar{\bar{D}}_B$ of 62.3 Gy. The total control probability, P_B, is 74.1% and the total complication probability, P_I, is 3.3%. Finally, for the HT plan, the P_+ value is 66.8% for $\bar{D}_{ITV} = 64.3$ Gy and $\bar{\bar{D}}_B$ of 64.3 Gy. The total control probability, P_B, is 77.4% and the total complication probability, P_I, is 10.6%. In every case, the prescribed doses are quite close to the optimum dose level, which maximizes the complication-free tumor control. At this optimum dose level, for the 3D-conformal plan the P_+ value becomes 55.4% for a $\bar{\bar{D}}_B$ of 57.0 Gy having $P_B = 64.3\%$ and $P_I = 9.0\%$. Respectively, for the MLC-based IMRT the P_+

Table 2. Summary of the radiobiological evaluation and comparison of the 3D-conformal, MLC-based IMRT and HT treatment plans. The indices C, P and T refer to Conformal, Pinnacle and Tomotherapy

Tissue	P_C (%)	P_P (%)	P_T (%)	$\bar{\bar{D}}_C$	$\bar{\bar{D}}_P$	$\bar{\bar{D}}_T$	$\bar{D}_C$	$\bar{D}_P$	$\bar{D}_T$	SD_C	SD_P	SD_T	Dmax C	*Dmax* P	*Dmax* T	*Dmin* C	*Dmin* P	*Dmin* T
ITV*	72.6	74.1	77.4	61.3	62.3	64.3	61.4	62.4	64.3	1.8	2.1	0.6	65.4	66.2	67.6	54.4	53.9	62.2
Spinal cord	~0.0	~0.0	~0.0	48.5	48.8	48.5	19.4	22.3	16.6	16.3	16.0	11.9	47.4	49.5	42.3	0.3	0.3	0.7
Esophagus	15.4	2.5	8.6	59.7	55.5	58.0	33.9	23.5	20.5	23.5	10.7	11.5	63.1	61.4	65.5	5.7	2.0	2.4
Heart	~0.0	~0.0	~0.0	17.9	18.6	16.5	5.5	6.5	6.9	6.9	8.7	7.5	47.1	38.2	36.2	0.3	0.3	0.3
Ipsilateral lung	8.3	0.8	2.2	23.0	15.2	18.0	19.1	12.8	15.5	21.8	16.0	16.7	65.4	65.9	66.2	0.3	0.3	0.3

Radiation modality	*Conformal radiotherapy*		*MLC-based IMRT*		*Helical tomotherapy*	
Dose prescription	*Clinical*	*Optimum* P_+	*Clinical*	*Optimum* P_+	*Clinical*	*Optimum* P_+
P_+ (%)	50.0	55.4	70.9	72.9	66.8	66.9
P_B (%)	72.6	64.3	74.1	80.9	77.4	76.7
P_I (%)	22.5	9.0	3.3	7.9	10.6	10.1
$\bar{\bar{D}}_B$ (Gy)	61.3	57.0	62.3	66.9	64.3	64.0
$\bar{\bar{D}}_I$ (Gy)	28.3	23.3	19.4	22.7	24.1	23.8

*internal target volume

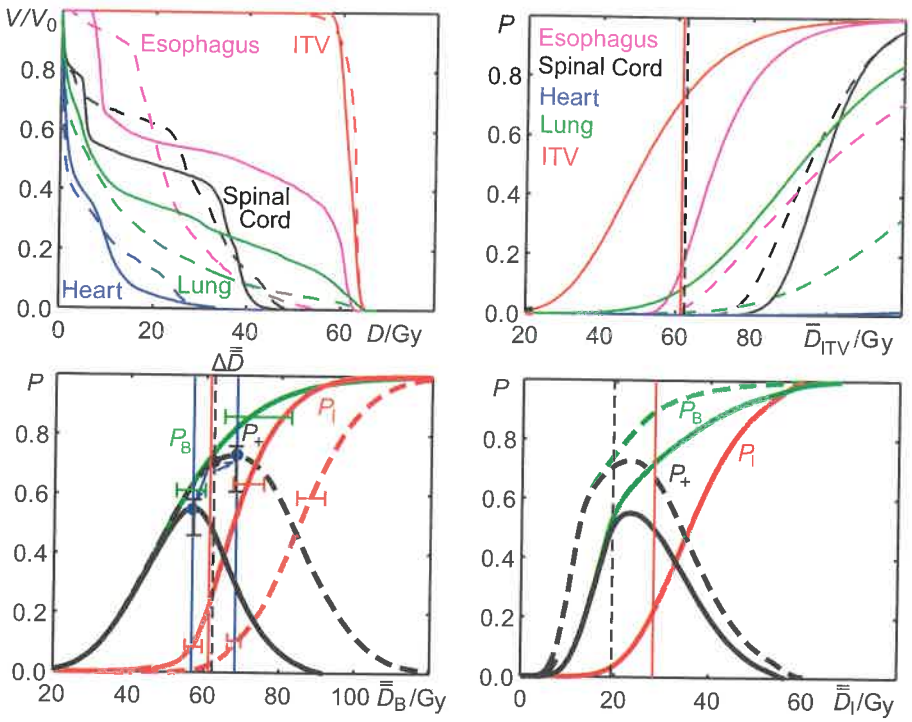


Figure 2. Lung cancer case. Conformal: solid line, IMRT: dashed line. In the upper left diagram, the DVHs of the ITV and those of the organs at risk (spinal cord, esophagus, heart and ipsilateral lung) are shown. In the right diagrams, the prescription dose levels are presented. The curves that are derived from the radiobiological evaluation of the two treatment plans are plotted in the same diagram using the mean dose to the ITV (upper right diagram) and $\bar{\bar{D}}$ (lower diagrams) on the dose axis.

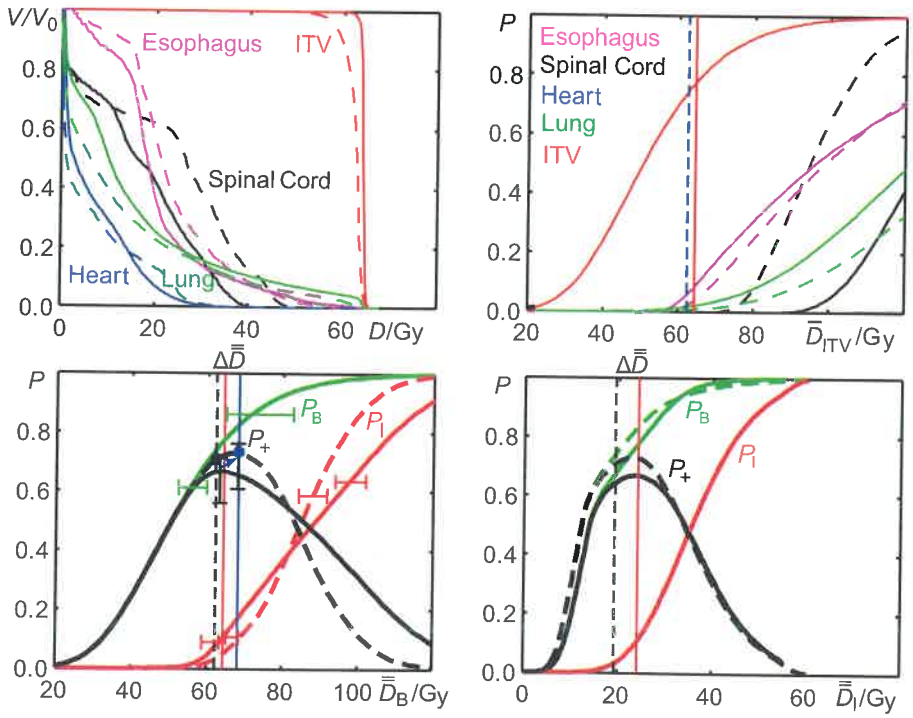


Figure 3. Lung cancer case. Tomotherapy: solid line, IMRT: dashed line. In the upper left diagram, the DVHs of the ITV and those of the organs at risk (spinal cord, esophagus, heart and ipsilateral lung) are illustrated. In the right diagrams, the prescription dose levels are presented. The dose-response curves of the two radiation modalities are plotted in the same diagram using the mean dose to the target and the $\bar{\bar{D}}$ on the dose axis.

value becomes 72.9% for a $\bar{\bar{D}}_B$ of 66.9 Gy having P_B = 80.9% and P_I = 7.9%. Finally, for the HT plan the P_+ value becomes 66.9% for a $\bar{\bar{D}}_B$ of 64.0 Gy having P_B = 76.7% and P_I = 10.1%.

A more schematical description of the radiobiological evaluation of the 3 treatment plans is presented in Figures 2 and 3. It is shown that both the HT and MLC-based IMRT dose distributions are characterized by a high conformality to the ITV sparing very well the OARs involved. At the prescribed dose level of the distributions, the mean doses to the ITV are high and very close to the optimum level, which would maximize their control with a good compensation for normal tissue complications. The latter characteristic does not hold for the conformal 3D treatment plan, where the expected complications of the esophagus and lung are significantly high. With the exception of the esophagus, in the HT treatment plan, the mean and maximum doses in the organs at risk are low ensuring low levels of expected complications. For all the 3 plans, the maximum doses of the esophagus and lung appear to be elevated because of their proximity to the ITV.

Discussion

In this study, a lung cancer case was investigated in order to evaluate the clinical effectiveness of 3D-conformal, MLC-based IMRT and Helical Tomotherapy using both physical and radiobiological measures. Criteria such as the mean and minimum target dose, normal tissue tolerance doses, isodose levels and DVHs were mostly used in the physical analysis of the 3 treatment plans [1]. More specifically, the uniformity of the dose distribution in the target volume and the dose level constraints were the basis for the evaluation and classification of the different radiation modalities. The ITV should receive at least a certain minimum dose specified by the clinical protocols, while the tolerance doses of the involved organs at risk should not be reached. The 3D-conformal radiation modality delivers high dose to a large volume. The ITV is covered with the preferred isodose curve but the esophagus and lung are not protected well. In the linac-based IMRT and HT plans, the ITV is covered sufficiently well by the dose distributions. However, the MLC-based IMRT spares a little better the esophagus and lung compared to the HT, while all the other OARs are spared very well.

Pinnacle and Tomotherapy treatment planning systems use different prescription techniques and delivery modalities in producing their dose matrices. The HT unit has a 64 leaf binary MLC to deliver radiation from 51 beam angles per rotation. In this case, instead of the whole tumor being covered by an isodose curve, each voxel inside the tumor will receive a homogeneity dose. The step-and-shoot IMRT plan uses a millennium 120 leaf MLC to deliver the intensity map with 9 beam angles, as prescribed to the calculation point. Results show that HT and MLC-based IMRT may produce dose distributions with fairly homogeneous doses to the ITV and small integral doses to the healthy organs.

In the literature, there are some recent studies regarding the comparison of HT against conventional conformal treatment techniques as well as of HT against IMRT in treating lung cancer [36]. However, these studies performed only dosimetric comparisons between the different radiation modalities without showing what is the impact of the observed differences on the expected treatment outcome, which is the final goal of treatment planning. This important gap in the assessment of the clinical effectiveness of the different modalities is covered by the present study, which interprets the dosimetric characteristics of the 3 different treatment plans into expected rates of tumor control and normal tissue complications.

In the comparisons between the 3D-conformal, MLC-based IMRT and HT treatment plans, the differences observed on the DVHs are not always reflected in the radiobiological evaluation. This is because different dose-response relations, expressing the radiobiological characteristics of different tissues, are affected in different ways by a certain dose distribution. Similarly, two dose distributions may have the same mean dose and standard deviation but different response probabilities when irradiating the same tissue. In the lower left diagrams of Figures 2 and 3, where the $\bar{\bar{D}}_B$ is used, it is shown that the curves corresponding to the response of the ITV (P_B) coincide. In this way, the classification and superiority of the plans are determined by comparing the response curves of the organs at risk. Similarly, the $\bar{\bar{D}}_I$ is used as the dose level unit in the lower right diagrams. This unit forces the response curves, which correspond to the total complication probabilities, P_I to lie at the same position for the different plans. Consequently, the classification and superiority of the plans are determined by comparing the control curves. By using these kinds of diagrams, it is observed how the control probability changes when certain complication thresholds are examined. The $\bar{\bar{D}}$ concept is based on the fact that a 3D dose distribution may be reduced to a single dose causing the same response probability. The use of the mean dose delivered to the ITV does not provide a common dose scaling basis for comparison of different plans. That is because for the same control rate, different mean doses to the ITV are delivered by different plans and by using this scale it is harder to

compare the effect of the treatment to the rest of the involved organs (Figures 2 and 3, upper right diagrams). This evaluation procedure could be used as a guide for treatment plan evaluation and dose prescription. Furthermore, it can be the ultimate tool for verifying published clinical parameters and comparing dose escalation studies. The biological evaluation plot of a dose plan is a good illustration of the expected clinical outcome, as the dose volume histogram chart is a good illustration of the volumetric dose distribution delivered to the patient. Using the dose-response diagrams together with the dosimetric diagrams, a more complete picture of the delivered treatment is given.

As shown in Figure 2, the expected complication-free tumor control for the MLC-based IMRT treatment plan is better than the 3D-conformal plan over the whole range of clinical prescribed doses, whereas the HT treatment plan is worse (Figure 3) than the MLC-based IMRT for prescribed doses between 55-80 Gy. The reason for this is that although the HT irradiates the ITV a little more effectively, the MLC-based IMRT dose distribution gives better sparing to the esophagus and lung, which makes it the superior plan as shown in Table 2 and the upper diagrams of Figure 3, where the individual DVHs and response curves of all the tissues are illustrated. In comparison with the 3D-conformal plan, both the MLC-based IMRT and HT plans show higher target control and much lower complication probabilities. It should be mentioned that although HT delivers lower mean dose to the esophagus with a little larger standard deviation compared to the MLC-based IMRT, it shows a significantly higher complication probability because of its greater maximum dose and the high relative seriality value of esophagus. The same holds for the 3D-conformal plan, which delivers to the esophagus a high mean dose as well as a high maximum dose. For the lung, which is a parallel organ (being characterized by a low relative seriality value), the higher mean dose delivered by the 3D-conformal plan is the dominating factor for the large complication probability (8.3%). In this case, although the dose variation is large, the $\bar{\bar{D}}$ value does not deviate much from the corresponding mean dose, $\bar{D}$, because of the low relative seriality values that characterize lung tissue. In tissues of parallel internal organizations, dose inhomogeneity does not affect so much their response, which is mainly determined by the mean dose. The better results of the MLC-based IMRT compared to those of the HT plan partly stem from the fact that the Pinnacle TPS offers the possibility for a radiobiological treatment plan evaluation and optimization, whereas the HT TPS has not yet developed such a module, which may guide the optimization code to improve a little more the final dose distribution. Evaluations and comparisons of this type cannot be done using only the physical data of the treatment plans.

In the lower diagrams of Figures 2 and 3, the clinically established dose prescription, which corresponds to a certain uniform dose in the gross tumor, is shown to deviate from the optimal dose level that the radiobiological evaluation provides for the 3 treatment plans. In Table 2, it is observed that in the case of the MLC-based IMRT plan, the planned dose prescription is lower than the optimum. This is because at the planned (prescribed) level of the dose distribution, an acceptable compromise has been achieved. However, when the radiobiological data of the different tissues are available, then it can be seen that there is a margin of improvement. By a small increase in the dose prescription, the gain in tumor control is larger than the increase in normal tissue complications until a balance is reached. Because of these points the clinically prescribed dose level is lower than the optimum level by a $\Delta\bar{\bar{D}}$ of 4.6 Gy. In the case of the 3D-conformal treatment plan, the planned dose prescription is higher than the optimum dose level by a $\Delta\bar{\bar{D}}$ of -4.3 Gy. This is because in order to ensure a high tumor control probability, a quite high risk for normal tissue complications had to be accepted. However, the radiobiological evaluation showed that by lowering the level of the dose distribution the complication rate dropped much more than the tumor control rate until a point of balance was reached. Finally, in the case of the HT plan, the planned dose prescription is almost the same with the optimum dose level ($\Delta\bar{\bar{D}}$ = -0.3 Gy).

In the diagrams of the dose volume histograms of Figures 2 and 3, the boost to the more radioresistant ITV is observed. For the MLC-based IMRT and HT plans, the organs at risk receive quite low doses and their response curves are well separated from the ones of the targets. This broadens the therapeutic window of the treatment leading to better expected clinical outcome as it is shown in the diagram with the results of the radiobiological evaluation (upper right diagrams). It can also be seen that as the curve of P_+ becomes higher the width of the therapeutic window broadens [37]. The width of the P_+ curve expresses the separation between the response curves of the tumors and the involved normal tissues. The width of the therapeutic window also gives an indication of how robust the treatment plan is against dose delivery and patient radiosensitivity uncertainties. The present analysis shows that in the optimization of the treatment planning process, P_+ can be a valuable parameter. The clinical evaluation of a certain dose distribution and the optimization of its dose level can be performed by the use of the com-

plication-free tumor control index. At the same time, since the most conformal treatment plan generates a higher value of P_+, the optimum treatment modality is indicated. Instead of just optimizing physical functions, the use of this method is a rather good way for making use of the patient specific characteristics. In this way, difficult clinical situations could be overcome and good, reliable treatment plans that would provide better survival probabilities for the patient and perhaps a better quality of life could be found. In these diagrams, the radiobiological information of the organs involved in the clinical case are combined with the dosimetric information of the delivered dose distribution.

It has been shown that radiation doses to OARs can be significantly limited when using IMRT. However, when CTV is adjacent to highly radiosensitive critical organs, the ITV expansion often does not allow for much organ sparing. Margin expansion of the GTV and CTV as well as dose escalation possibilities are allowed by preferential OAR sparing. Dose inhomogeneity within an organ is generally associated with the delivery of different daily radiation doses to different regions. The effect of this inhomogeneity is to produce a concurrent radiation local boost that will give a higher total radiation dose to a limited region [38]. Although a very accurate setup can be provided by taking a CT immediately before each treatment fraction, normal organ motion during a treatment session is not taken into account [39]. Respiratory gating and active breath hold techniques have been developed for the 3D-conformal and MLC-based IMRT radiation modalities but not for the HT [40,41]. In many cases, during treatment delivery, organs such as liver, pancreas and kidneys may move in and out of the ITV due to normal respiration, while tumor bed is not expected to significantly change position. The need for a quite large setup margins may limit the opportunity to achieve the goals of dose escalation and target volume expansion. The amount of movement during quiet respiration might be assumed to be less than during full inspiration and expiration, but the few published studies give quite variable results. During quiet respiration, the amount of movement in the cranio-caudal axis may be up to 20 mm.

One of the key points of the paper is the usefulness of $P-\bar{\bar{D}}$ diagrams. These diagrams combine the dosimetric information of the delivered dose distribution with the radiobiological information of the organs involved in each clinical case. The definition of the P_+ concept does not precisely depict the clinical way of thinking. It would be more reasonable if the different terms related to the tumor control and normal tissue complication probabilities were accompanied by some weighting factors, which could be adjustable by the clinicians. The above mentioned diagrams can be used in conjunction with the P_+ curve, but not necessarily. By using the $\bar{\bar{D}}$ concept on the dose axis, the control and complication probabilities of the different targets and OARs can be examined individually. The major advantage is that the $\bar{\bar{D}}$ concept forces the total control or total complication probabilities of different plans to coincide and the comparison of the response curves becomes much simpler than when the mean target dose is used.

The results and conclusions of this study are strongly dependent on the accuracy of the radiobiological models and the parameters describing the dose-response relation of the different tumors and normal tissues. However, it is known that all the existing models are based on certain assumptions or take into account only certain biological mechanisms. Furthermore, the determination of the model parameters expressing the effective radiosensitivity of the tissues is subjected to uncertainties imposed by the inaccuracies in the patient setup during radiotherapy, lack of knowledge of the inter-patient and intra-patient radiosensitivity and inconsistencies in treatment methodology [42-44]. Consequently, the determined model parameters (such as the D_{50} γ and s) and the corresponding dose-response curves are characterized by confidence intervals. In the present study, most of the tissue response parameters have been taken from recently published clinical studies, where these parameter confidence intervals have been reduced significantly (e.g. uncertainty of around 5% in the determination of D_{50}). So, the expected response of a tissue is known with some uncertainty, which has become clinically acceptable for many cancer sites. In the lower left diagrams of Figures 2 and 3, the confidence intervals of the P_B, P_I and P_+ response curves have been calculated and it can be observed that this uncertainty in the absolute knowledge of the expected responses does not affect the general conclusions of the study.

It is recognized that only one case of a single treatment site was used in this work. A statistically significant sample of cases would give a more accurate picture of the comparisons. However, for each of the 3 clinical cases presented, the treatment plans were produced using optimization algorithms, which calculated the final dose distributions based on some predefined criteria (inverse physical optimization). So, although a strict inter-modality comparison cannot be performed, an indication of the effectiveness of the 2 radiation modalities can be given. General conclusions about which treatment method is better are outside the scope of this paper. However, apart from the 3D-conformal radiation modality, both the MLC-based IMRT and HT modalities

appear to have similar possibilities in producing highly conformal dose distributions. Possibly, the very large number of degrees-of-freedom that characterizes the radiobiologically guided IMRTs makes it difficult to find a clear difference between them [45]. The potentially superior radiobiological results of the MLC-based IMRT and HT compared to the 3D-conformal modality can be even better demonstrated by using more severe endpoints in normal tissue complications. Furthermore, the findings of this paper show that the P_+ and $\bar{\bar{D}}$ concepts are very useful in comparing IMRT plans and they can give preference for selecting a better treatment plan. The presented $(P - \bar{\bar{D}})$ diagrams can be considered as the radiobiological version of the extensively used DVH diagrams.

Conclusion

In this study, the clinical effectiveness of a simple 3D-conformal, HT and MLC-based IMRT was evaluated for a lung cancer case. Using both physical and biological criteria, this evaluation showed that the 3D-conformal radiation modality has a poor expected clinical outcome as compared to the HT and MLC-based IMRT plans. The difference between the HT and MLC-based IMRT plans was small with the latter one being more effective over the clinically prescribed dose region. This work indicates that treatment plans with small integral doses to the healthy organs and fairly homogeneous doses to the ITV can be equally produced by both the HT and MLC-based IMRT radiation modalities. The application of the P_+ and $\bar{\bar{D}}$ concepts on the representative 3D-conformal, MLC-based IMRT and HT treatment plans of a lung cancer case revealed differences in the expected therapeutic impact of the 3 radiation modalities.

References

1. Aaltonen P, Brahme A, Lax I, Levernes S, Näslund I, Reitan JB, Turesson I. Specification of dose delivery in radiation therapy. Recommendations by the Nordic Association of Clinical Physics (NACP). Acta Oncol 1997; 36 (Suppl 10): 1-32.
2. ICRU report 62. Prescribing, recording and reporting photon beam therapy (supplement to ICRU report 50). International Commission on Radiation Units and Measurements 1999; 1-52.
3. Mavroidis P, Lind BK, Van Dijk J et al. Comparison of conformal radiation therapy techniques within the dynamic radiotherapy project "Dynarad". Phys Med Biol 2000; 45: 2459-2481.
4. Mavroidis P, Lind BK, Brahme A. Biologically effective uniform dose ($\bar{\bar{D}}$) for specification, report and comparison of dose response relations and treatment plans. Phys Med Biol 2001; 46: 2607-2630.
5. Källman P, Lind BK, Brahme A. An algorithm for maximizing the probability of complication free tumor control in radiation therapy. Phys Med Biol 1992; 37: 871-890.
6. Mackie TR, Balog J, Ruchala KJ et al. TomoTherapy. Semin Radiat Oncol 1999; 9: 108-117.
7. Webb S. Intensity-Modulated Radiation Therapy. Bristol: IOP Publishing; 2000.
8. Scrimger RA, Tome WA, Olivera GH, Reckwerdt PJ, Mehta MP, Fowler JF. Reduction in radiation dose to lung and other normal tissues using helical tomotherapy to treat lung cancer, in comparison to conventional field arrangements. Am J Clin Oncol 2003; 26: 70-78.
9. Bauman G, Yartsev S, Coad T, Fisher B, Kron T. Helical TomoTherapy for craniospinal radiation. Br J Radiol 2005; 78: 548-552.
10. Brahme A. Which parameters of the dose distribution are best related to the radiation response of tumours and normal tissues? In: Proceedings of the Interregional Seminars for Europe, the Middle East and Africa Organized by the IAEA, Leuven, 1994: 37-58.
11. Emami B, Lyman J, Brown A et al. Tolerance of normal tissue to therapeutic irradiation. Int J Radiat Oncol Biol Phys 1991; 21: 109-122.
12. Ågren AK. Quantification of the response of heterogeneous tumors and organized normal tissues to fractionated radiotherapy (Ph.D. Thesis). Stockholm University, 1995.
13. Mavroidis P, Laurell G, Kraepelien T, Fernberg JO, Lind BK, Brahme A. Determination and clinical verification of dose-response parameters for esophageal stricture from head and neck radiotherapy. Acta Oncol 2003; 42: 865-881.
14. Mavroidis P, al-Abany M, Helgason AR et al. Dose-response relations for anal sphincter regarding faecal leakage and blood or phlegm in stools after radiotherapy for prostate cancer. Strahlenther Onkol 2005; 181: 293-306.
15. Papanikolaou N, Shi C. A useful tool for trial comparison and developing composite plan between Tomotherapy and Pinnacle. Med Phys 2006; 33: 2065.
16. Papanikolaou N, Mackie TR, Meger-Wells C, Gehring M, Reckwerdt P. Investigation of the convolution method for polyenergetic spectra. Med Phys 1993; 20: 1327-1336.
17. Mackie TR, Scrimger JW, Battista JJ. A convolution method of calculating dose for 15-MV x rays. Med Phys 1985; 12; 188-196.
18. Ågren-Cronqvist AK, Brahme A, Turesson I. Optimization of uncomplicated control for head and neck tumors. Int J Radiat Oncol Biol Phys 1990; 19: 1077-1085.
19. Källman P, Ågren AK, Brahme A. Tumor and normal tissue responses to fractionated non uniform dose delivery. Int J Radiat Biol 1992; 62: 249-262.
20. Jackson A, Ten Haken RK, Robertson JM, Kessler ML, Kutcher GJ, Lawrence TS. Analysis of clinical complication data for radiation hepatitis using a parallel architecture model. Int J Radiat Oncol Biol Phys 1995; 31: 883-891.
21. Gagliardi G, Björhle J, Lax I et al. Radiation pneumonitis after breast cancer irradiation: Analysis of the complication probability using the relative seriality model. Int J Radiat Oncol Biol Phys 2000; 46: 373-381.
22. Lind BK, Mavroidis P, Hyödynmaa S, Kappas C. Optimization of the dose level for a given treatment plan to maximize the complication free tumor cure. Acta Oncol 1999; 38: 787-798.

23. Burman C, Kutcher GJ, Emami B et al. Fitting of normal tissue tolerance data to an analytical function. Int J Radiat Oncol Biol Phys 1991; 21: 123-135.
24. Kutcher GJ, Burman C, Brewster L, Goitein M, Mohan R. Histogram reduction method for calculating complication probabilities for 3-dimensional treatment planning evaluations. Int J Radiat Oncol Biol Phys 1991; 21: 137-146.
25. Kwa S, Theuws C, Wagendar A et al. Evaluation of two dose-volume histogram reduction models for the prediction of radiation pneumonitis. Radiother Oncol 1998; 48: 61-69.
26. Boersma LJ, Damen EM, De Boer RW. Estimation of overall pulmonary function after irradiation using dose-effect relations for local functional injury. Radiother Oncol 1995; 36: 15-23.
27. Eriksson F, Gagliardi G, Liendberg A et al. Long-term cardiac mortality following radiation therapy for Hodgkin's disease: analysis with the relative seriality model. Radiother Oncol 2000; 55: 153-162.
28. Roesink JM, Moerland MA, Battermann JJ, Hordijk GJ, Terhaard CHJ. Quantitative dose–volume response analysis of changes in parotid gland function after radiotherapy in the head-and-neck region. Int J Radiat Oncol Biol Phys 2001; 51: 938-946.
29. Willner J, Baier K, Caragiani E, Tschammler A, Flentje M. Dose, volume, and tumor control predictions in primary radiotherapy of non-small-cell lung cancer. Int J Radiat Oncol Biol Phys 2002; 52: 382-389.
30. Tsougos I, Nilsson P, Theodorou K et al. NTCP modeling and pulmonary function tests evaluation for the prediction of radiation induced pneumonitis in non-small-cell lung cancer radiotherapy. Phys Med Biol 2007; 52: 1055-1073.
31. Deasy JO (Ed). Inter-patient and intra-tumor radiosensitivity heterogeneity. In: Volume and Kinetics in Tumor Control and Normal Tissue Complications. Madison, WI: Medical Physics Publishing, 1997, pp 363-381.
32. Brahme A. Dosimetric precision requirements in radiation therapy. Acta Radiol Oncol 1984; 23: 379-391.
33. Niemierko A. Reporting and analysing dose distributions: A concept of equivalent uniform dose. Med Phys 1997; 24: 103-110.
34. Brahme A. The need for accurate target and dose specifications in conventional and conformal radiation therapy - An introduction. Acta Oncol 1997; 36: 789-792.
35. Kölbl O, Richter S, Flentje M. Influence of treatment technique on dose-volume histogram and normal tissue complication probability for small bowel and bladder. Strahlenther Onkol 2000; 176: 105-111.
36. Kron T, Grigorov G, Yu E et al. Planning evaluation of radiotherapy for complex lung cancer cases using helical tomotherapy. Phys Med Biol 2004; 49: 3675-3690.
37. Brahme A. Development of radiation therapy optimization. Acta Oncol 2000; 39: 579-595.
38. Pezner RD, Liu A, Han C, Chen YJ, Schultheiss TE, Wong JYC. Dosimetric comparison of helical tomotherapy treatment and step-and-shoot intensity-modulated radiotherapy of retroperitoneal sarcoma. Radiother Oncol 2006; 81: 81-87.
39. Papanikolaou N, Yan Y, Penagaricano J, Ratanatharathorn V. The impact of daily patient setup error and tissue inhomogeneity on PTV coverage and OAR avoidance using IMRT. Med Phys 2002; 29: 1286.
40. Lind BK, Källman P, Sundelin B, Brahme A. Optimal radiation beam profiles considering uncertainties in beam patient alignment. Acta Oncol 1993; 32: 331-342.
41. Löf J, Lind BK, Brahme A. Optimal radiation beam profiles considering the stochastic process of patient positioning in fractionated radiation therapy. Inverse Problems 1995; 11: 1189-1209.
42. Buffa FM, Davidson SE, Hunter RD et al. Incorporating biologic measurements (SF2, CFE) into a tumor control probability model increases their prognostic significance: A study in cervical carcinoma treated with radiation therapy. Int J Radiat Oncol Biol Phys 2001; 50: 1113-1122.
43. Fenwick JD, Nahum AE. Series model volume effects in a population of non-identical patients: how low is low? Phys Med Biol 2001; 46; 1815-1834.
44. Nahum AE, Movsas B, Horwitz EM, Stobbe CC, Chapman JD. Incorporating clinical measurements of hypoxia into tumor local control modeling of prostate cancer: implications for the alpha/beta ratio. Int J Radiat Oncol Biol Phys 2003; 57: 391-401.
45. Ferreira BC, Svensson R, Löf J, Brahme A. The clinical value of non-coplanar photon beams in biologically optimized intensity modulated dose delivery on deep seated tumors. Acta Oncol 2003; 42: 852-864.